DTU Library

A gain-loss framework based on ensemble flow forecasts to switch the urban drainage-wastewater system management towards energy optimization during dry periods

Courdent, V.; Grum, M.; Munk-Nielsen, T.; Mikkelsen, Peter Steen

Link back to DTU Orbit

A gain–loss framework based on ensemble flow forecasts to switch the urban drainage–wastewater system management towards energy optimization during dry periods

Vianney Courdent[1,2], Morten Grum[1,a], Thomas Munk-Nielsen[1], and Peter S. Mikkelsen[2]

[1]Krüger Veolia, Søborg, 2860, Denmark
[2]Department of Environmental Engineering, Technical University of Denmark, Kgs. Lyngby, 2800, Denmark
[a]present address: WaterZerv, Environmental Services, Denmark

Correspondence to: Vianney Courdent (vatc@env.dtu.dk)

Abstract. Precipitation is the cause of major perturbation to the flow in urban drainage and wastewater systems. Flow forecasts, generated by coupling rainfall predictions with a hydrologic runoff model, can potentially be used to optimize the operation of integrated urban drainage–wastewater systems (IUDWSs) during both wet and dry weather periods. Numerical weather prediction (NWP) models have significantly improved in recent years, having increased their spatial and temporal resolution. Finer resolution NWP are suitable for urban-catchment-scale applications, providing longer lead time than radar extrapolation. However, forecasts are inevitably uncertain, and fine resolution is especially challenging for NWP. This uncertainty is commonly addressed in meteorology with ensemble prediction systems (EPSs). Handling uncertainty is challenging for decision makers and hence tools are necessary to provide insight on ensemble forecast usage and to support the rationality of decisions (i.e. forecasts are uncertain and therefore errors will be made; decision makers need tools to justify their choices, demonstrating that these choices are beneficial in the long run).

This study presents an economic framework to support the decision-making process by providing information on when acting on the forecast is beneficial and how to handle the EPS. The relative economic value (REV) approach associates economic values with the potential outcomes and determines the preferential use of the EPS forecast. The envelope curve of the REV diagram combines the results from each probability forecast to provide the highest relative economic value for a given gain–loss ratio. This approach is traditionally used at larger scales to assess mitigation measures for adverse events (i.e. the actions are taken when events are forecast). The specificity of this study is to optimize the energy consumption in IUDWS during low-flow periods by exploiting the electrical smart grid market (i.e. the actions are taken when no events are forecast). Furthermore, the results demonstrate the benefit of NWP neighbourhood post-processing methods to enhance the forecast skill and increase the range of beneficial uses.

1 Introduction

The primary objective of combined urban drainage systems (UDSs) and wastewater treatment plants (WWTPs) is to convey and treat waste water and to prevent flooding and combined sewer overflows (CSOs). In order to achieve these objectives, pipes and detention basins in combined UDSs are dimensioned to cope with relatively large rain events. Typically, surcharge of manholes and flooding is only allowed to occur on average every 10 years (as per the Danish regulations; Harremoës et al., 2005) whereas overflow occurs more frequently depending on the local environmental regulations, from 10 times per year to once in 10 years, for example. This means that during dry weather the flow is relatively low compared with the conveyance capacity of the UDS and that the storage capacity is left unused. Rainfall only occurs rarely, e.g. on the study case catchment (more details in Sect. 2.3.)

the raining period represents 7.2 % of the time. Hence, integrated urban drainage–wastewater systems (IUDWSs) are mostly under low-flow conditions. During these periods the IUDWS management objective can be switched from its priority operational focus on CSO and flood prevention towards other goals such as energy consumption and CO_2 emissions.

Denmark has the political ambitions to have a fossil fuel free energy system by 2050 which requires the development of renewable energy sources (Ministry of Foreign Affairs of Denmark, 2016). One of the main critiques towards renewable sources such as wind and solar energy is their intermittent nature. Therefore a key parameter for the transition to a green energy system is the implementation of an electric smart grid with flexible, proactive consumers to balance the fluctuating power production (Hadjsaïd and Sabonnodiere, 2012). The European Technology Platform for smart grids defines the concept of smart grids as an "electricity network that can intelligently integrate the actions of all users connected to it – generators, consumers and those that do both – in order to efficiently deliver sustainable, economic and secure electricity supplies" (www.smartgrids.eu/). Energy markets are developed, as part of the smart grid, to align electricity production and consumption through bids and offers. Hence the electricity price is based on supply and demand, creating an economic incentive to distribute the energy consumption in time (e.g. shifting non-essential energy consumption out of the consumption peaks). For further detailed history and description of electricity markets, see Weron (2006).

IUDWS can potentially be used actively to take advantage of the energy market variation. Wastewater, for example, contains organic matter which can be converted to biogas at the WWTP, and the biogas production process may provide some energy storage that is potentially useful in a smart grid context. Furthermore, during dry periods, the unused storage in the UDS can be used as a buffer to control the timing of the energy consumption associated with wastewater transportation and treatment. Figure 1 highlights that both wastewater production and energy consumption are driven by human activities and therefore have similar daily pattern. This means that the energy is generally more expensive when the need for wastewater transportation and treatment is peaking. The energy market is also influenced by other parameters (e.g. the solar and wind intensity) but on yearly average the impact of the daily consumption can be observed.

Aymerich et al. (2015) investigated the relation between the energy consumption and energy cost at a WWTP in regard to energy tariff structures (i.e. energy markets). The aeration process represents between 50 and 70 % of the WWTP process energy consumption (Rosso and Stenstrom, 2005). Leu et al. (2009) studied the impact of a varying wastewater load on the oxygen transfer efficiency and aeration costs, considering to the daily variation of the power rates, and showed that there is potential to reduce the average power costs, within the limitations of the WWTP storage capacity.
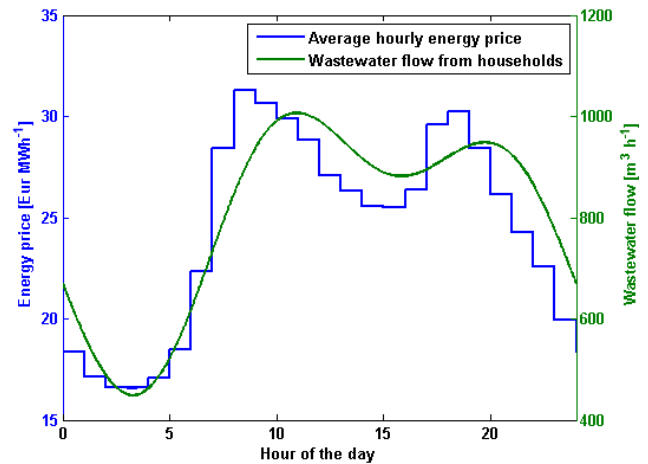

Figure 1. Yearly average (2015) of hourly energy price for the energy market DK2 covering the Copenhagen region (in blue, data from http://www.nordpoolspot.com/). Calibrated daily variation of the dry weather flow for the Damhuså catchment (green) used for demonstration in this paper; see further details in Sect. 2.3.

Bjerg et al. (2015) investigated the use of the storage volume in the pipe system upstream from a WWTP in Kolding (Denmark) to store wastewater and utilize the energy price fluctuations. However, such optimization requires information on the incoming loads (i.e. flow predictions), in order to know when it is safe to optimize the energy consumption (i.e. when the weather is dry) and when to prepare and operate the IUWDS to cope with large inflows during wet weather. Such flow predictions should ideally cover the forecast horizon of the smart grid market, i.e. 1 to 2 days (e.g. the day-ahead energy market; Zugno, 2013), which requires the use of numerical weather prediction (NWP) models.

NWPs are already in use in other fields such as wind and solar power production prediction (Bacher et al., 2009; Giebel et al., 2005), streamflow forecasting (Cuo et al., 2011; Shrestha et al., 2013), reservoir inflow prediction (Collischonn et al., 2007), flood forecasting (Damrath et al., 2000), and typhoon forecasting (Chang et al., 2015). Uncertainty is a challenge for NWP, especially for precipitation which is non-continuous and highly variable in both space and time. To tackle this problem, meteorologists commonly generate ensemble prediction systems (EPSs) by perturbing the initial conditions and the physics of the NWP models to generate a number of ensemble members (EMs) that represent an ensemble spread. The quality of an EPS can be quantitatively assessed based on various forecast characteristics. The relative operating characteristic (ROC; Mason, 1982) is used to measure the discrimination skill (i.e. the ability to discriminate between events and non-events) of an EPS, by plotting the empirical probability of detection (PoD) versus the probability of false detection (PoFD). Using an EPS increases the event discrimination skill by providing a larger range of predictions than an individual deterministic forecast.

The development of high-resolution limited-area NWP models has led to more realistic-appearing forecasts. Convective precipitations are described in an explicit and more detailed way using mesoscale atmospheric processes (Sun et al., 2014). These developments foster the opportunity of UDS applications which require fine temporal and spatial resolution. However, precipitation is one of the most difficult variables to forecast on an urban scale due to its large variability in space, time and intensity (Du, 2007). Precipitation forecast uncertainties increase rapidly with decreasing spatial grid size, as inevitable errors in the position and timing of rain cells are amplified with the increase in resolution. EPSs aim to describe this uncertainty, but are generally under-dispersive and unable to capture all sources of uncertainty. NWP post-processing methods (also called pre-processing from a hydrological modelling point of view) are thus necessary to obtain reliable probabilistic forecast as explained in WWRP/WGNE (2009). Courdent et al. (2017) described NWP post-processing methods for urban drainage flow forecasting and compared their event discrimination skills. The neighbourhood methods (Theis et al., 2005) can, for example, be used to enhance the forecast skill by accounting for potentially misplaced rain events. The "maximal threat" method NWP post-processing, used in this study, considered the highest rainfall prediction within a given area surrounding the catchment. The radius of the neighbouring area included is used as a parameter during the decision making, in addition to the fraction of EM f_{EM}.

This article presents a framework for objectively optimizing EPS forecast-based decision making in the management of IUDWSs by selecting the decision threshold f_{EM} and post-processing neighbourhood method, given the specific problem at hand. The relative economic value (REV) approach associates economic values to the outcomes of the decision system and assesses the forecast value relative to potential benefit resulting from a perfect forecast. The preferential management for a given EPS forecast is characterized by the highest REV. For example, we considered the decision-making problem of switching from normal operation focussing on flow management to dry weather operation focussing on energy optimization linking with the smart grid. To measure the usefulness of weather forecasts, the forecast skills have to be converted to potential economic benefits for the user decision making process. Richardson (2000) used the REV to assess the economic benefit of road gritting to prevent the formation of ice using weather models in comparison to using purely climatological information (i.e. the statistical behaviour of the weather, such as the return period of an event). Economic values were assigned to the different prediction outcomes described in a contingency table: (*a*) hits, (*b*) false alarms, (*c*) misses and (*d*) correct negatives. These economic values represent the benefit of taking actions (or non-action) when the forecast is revealed to be correct against the drawbacks of those actions (or non-action) in case of forecast error.

EPS provides a range of prediction skills characterized by the combined choice of post-processing method and decision threshold (f_{EM}) used to predict an event. The REV of each combination is quantified considering the occasions when the forecast proves to be beneficial, detrimental or neutral to the user, as well as the economic value associated with these situations. The higher the cost of inappropriate action relative to the potential gain, the more certainty the user requires about the forecast before he or she takes action.

Previous studies on REV analysis typically assessed the benefit of prevention measures mitigating severe weather events, such as frost (Richardson, 2000), intense precipitation (Atger, 2001), river floods (Roulin, 2007) and typhoons (Chang et al., 2015), expressed as a cost–loss ratio. This study develops a different perspective, assessing the potential benefit of optimizing IUDWS when the forecast predicts periods with low flow (i.e. dry weather when no events are forecast). Therefore, our decision model is not based on a cost–loss ratio but a gain–loss ratio. Furthermore, the studies mentioned consider a fixed ratio, whereas in our case (i) the gain depends on smart grid variations and (ii) the loss is related to the risk of CSO and the negative impact on the WWTP operation. Hence, the gain–loss ratio and the optimum combination of post-processing method and decision threshold need to be reassessed for each time step.

This paper is organized as follows: Sect. 2 introduces the DMI-HIRLAM-S05 weather model, which provides the rainfall forecast used in our study, the NWP post-processing method applied and the hydrological rainfall–runoff model. Section 3 describes the prediction performance evaluation methods used, including the ROC and the REV diagrams. Results and prediction examples are presented and discussed in Sect. 4. Finally, Sect. 5 provides the conclusions.

2 Material: NWP data, study case and hydrological model

As emphasized by Shrestha et al. (2013), the evaluation of NWP model precipitation forecasts for streamflow forecasting should be done with a hydrological perspective. Therefore, as recommended by Pappenberger et al. (2008), the evaluation of urban drainage flow forecasts is in this paper based on a coupled meteorological and hydrological model. Hence, the forecast skills are assessed based on discharge predictions and discharge observations rather than precipitation forecasts and precipitation observations. This methodology considers the importance of the dominant hydrological processes and the nonlinear error transformation by the hydrological model.

This section describes the NWP model and data used in the study. Then the post-processing neighbourhood methods are presented, the urban catchment study case is presented, the hydrological model is described, and finally the energy market data that was used is presented.

2.1 The EPS HIRLAM-DMI-S05 numerical weather prediction (NWP) model

The rainfall forecasts used in this study were generated by the DMI-HIRLAM-S05 model and were provided by the Danish Meteorological Institute (DMI). This NWP model has a horizontal resolution of 0.05° (approx. 5.6 km) and a forecast horizon of 54 h with hourly time-step predictions. New forecast are generated every 6 h, at 00:00, 06:00, 12:00 and 18:00 UTC. The DMI-HIRLAM-S05 ensemble is a 2-dimensional EPS comprising 25 members based on 5 different initial conditions and 5 different model structures. For further description of the processes and parameters mentioned above, see the HIRLAM technical documentation (Unden et al., 2002), the DMI technical report (Feddersen, 2009) and the HIRLAM website (http://www.hirlam.org/). This study uses 2 years of archived EPS NWP data (from June 2014 to May 2016).

2.2 Enhancing forecast by post-processing NWP EPS data

Two NWP post-processing methods developed in Courdent et al. (2017) were used in this study: (i) the realistic catchment "weighted areal overlap" method which only considers the grid cells overlapping the hydrologic catchment and weighs them based on the percentage of overlap and (ii) the maximal threat in the surroundings method, which considers cells within a defined radius around the catchment. The maximal threat method combines the worst-case-scenario approach and the neighbourhood method developed by Theis et al. (2005), and accounts for neighbourhood cells in the prediction as illustrated by Fig. 2. Hence, the maximal threat approach considers as input, for each EM, the highest rainfall intensity in the surroundings. This method keeps the same ensemble size as the weighted areal overlap method and reduces the number of missed events but increases the number of incorrectly predicted or over-predicted events.

2.3 Study case

The economic framework developed in this study was applied on the Damhuså urban drainage catchment (Copenhagen, Denmark). This 67 km^2 highly urbanized area composed of compact residential housing is equipped with a combined sewer system which conveys wastewater, rainfall runoff from paved surfaces and infiltration inflow, especially in the winter months. This catchment was chosen for the absence of major flow-control infrastructures affecting its hydraulic response in order to simplify the modelling approach needed for our demonstration. The Damhuså WWTP has a capacity of 350 000 PE (population equivalent). Its biological treatment has a maximal hydraulic capacity of 10 000 m^3 h^{-1}. In 2015, the WWTP treated 33 390 000 m^3 and consumed 8735 MWh of electricity, which correspond to
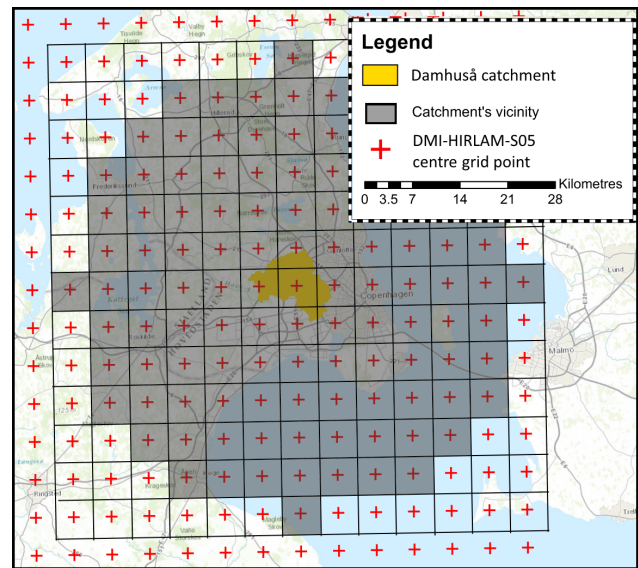

Figure 2. Illustration of the 6-grid-cell radius used by the maximal threat neighbourhood approach, for the Damhuså catchment used for demonstration in this paper (Courdent et al., 2017).

a ratio of 0.261 kWh m^{-3}. In parallel, the WWTP produced 8735 MWh of heat and 211 MWh of electricity from its biogas engine (BIOFOS, 2015).

Rainfall observation data were obtained from the national Danish SVK rain gauge network (blue circles in Fig. 3) which is operated by the Danish Meteorological Institute (DMI) and the Water Pollution Committee of the Danish Society of Engineers (SVK – Spildevandskomiteen, in Danish). The rainfall measurements were recorded with a 1 min temporal and a 0.2 mm volumetric resolution; for more information see Jørgensen et al. (1998). The catchment outlet (red hexagon in Fig. 3) is a combined sewer pipe interceptor with a maximum capacity of 10 000 m^3 h^{-1}. Once this threshold is reached, CSOs occur. The overflowing water is discharged, untreated, into a nearby small river (Damhuså) while the remaining flow is discharged through the interceptor pipe, which is monitored using an electromagnetic flow meter with a 2 min temporal resolution and operated by the utility company HOFOR.

This study is based on event prediction by characterizing the flow status in the IUDWS and distinguishing two domains: (i) periods with high flows during which the management objective is to maximize the hydraulic capacity of the WWTP to limit the impact of CSO, etc., and (ii) periods with low flows during which the management objectives can be switched to WWTP operational efficiency, minimizing energy consumption, etc. The event definition should be evaluated relatively to the specific IUDWS and low-flow optimization scheme in focus. In this study the occurrence of an event is defined by a flow exceedance of 4000 m^3 h^{-1} over a 1 h period. For each NWP the occurrence (or non-occurrence) of
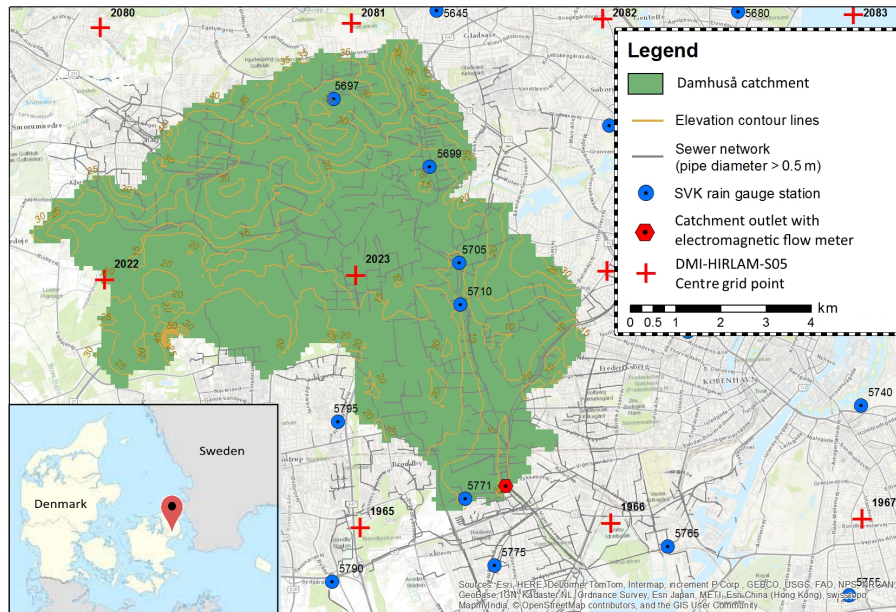
Figure 3. The Damhuså urban drainage catchment, Copenhagen, Denmark (contributing area: green area on the map).

a high-flow event is assessed for each hourly time step forecast.

2.4 Hydrological model description

The hydrological model is composed of three main conceptual parts: (i) the wastewater flow from households is modelled using second-order Fourier series (see, for example, Langergraber et al, 2008), (ii) the fast rainfall runoff from impervious areas is represented by a lumped conceptual model using the Nash linear reservoir cascade concept (Nash, 1957) and (iii) the slow runoff (caused e.g. by infiltration-inflow) is also modelled based on the Nash linear reservoir cascade concept using a wetness index characterized by the monthly potential evaporation and previous rainfall events. This hydrological model is further detailed in Courdent et al. (2017). The wastewater flow parameters were estimated first, using flow observations from summer periods without rainfall events to avoid influence from the two other processes. Then, using fixed wastewater parameters, the parameters of the fast rainfall runoff were estimated based on rain and flow data for rain events during summer months, to avoid influence from the slow runoff process, which was calibrated last for the full period (from November 2012 to November 2014). In all cases, the calibration was conducted using the differential evolution adaptive metropolis (DREAM) method (Laloy and Vrugt, 2012), considering the root mean square error as objective function.

2.5 Energy market data

This study used historical data from the day-ahead energy market provider Nord Pool. The day-ahead market has 24 h lead time. Buyers and suppliers submit bids and offers for each hour of the next day and each hourly market clearing price is set such that it balances supply and demand. The intra-day market, which only has 1 h lead time, is acting as a balancing market to support the day-ahead market. The hourly energy prices are defined over a geographical area. The geographical area corresponding to our case study is DK2 which covers the entire Zealand (http://www.nordpoolspot.com/).

3 Methodology

3.1 Contingency table

The probability that the flow will exceed a given threshold is estimated as the fraction of EMs predicting an event. The ensemble (probability) forecast can be converted to a single binary forecast by selecting a decision threshold (f_{EM}, threshold probability). If the fraction of EMs, predicting an event is higher or equal to the decision threshold (f_{EM}), then an event is forecast.

The empirical performance over a period of time of a binary forecast can be summarized in a 2×2 contingency table showing the number of correctly and incorrectly forecast events occurring or not occurring (Table 1). Hits (a) represent the correct positives, false alarms (b) represent the false positives, misses (c) represent the false negatives and the cor-

Table 1. Contingency table (with n the sample size).

Event forecast	Event observed		
	Yes	No	
Yes	hits (a)	false alarms (b)	$a+b$
No	misses (c)	correct negatives (d)	$c+d$
	$a+c$	$b+d$	$a+b+c+d=n$

Table 2. Verification measures based on the contingency table.

Score	Formula	Range	Perfect
Probability of detection, PoD	$a/(a+c)$	$[0,1]$	1
Probability of false detection, PoFD	$b/(b+d)$	$[0,1]$	0
Occurrence frequency of events, μ	$(a+c)/n$	$[0,1]$	n/a

n/a: not applicable.

rect negatives (d) represent the correct forecasts of no events occurring. Measures of performance of a sequence of binary forecasts can be formulated as a function of these four outcomes (a, b, c and d). Those four possible outcomes sum up to n, which corresponds to the total number of events assessed. Each event corresponds to the flow status of a given hourly time step forecast from a given NWP. The different lead times of the NWP are aggregated in the results.

Table 2 displays the verification measures used in this paper; a comprehensive review and further description of verification measures can be found in the meteorological literature, e.g. WWRP/WGNE (2009) and Wilks (2011).

The PoD is defined as the fraction of occurrences of events that were correctly forecast (i.e. hits), while the PoFD is the fraction of non-occurrences of events that were incorrectly forecast (i.e. false alarms). The empirical occurrence frequency (μ) expresses climatological information about the occurrence of events.

3.2 Brier skill score

The Brier score (Brier, 1950) assesses forecast quality of discrete probability forecasts predicting binary outcomes (i.e. "events" and "non-events") and is comparable to the mean square error. For a given tth hourly forecast time step, the forecast probability of an event ($0 \leq f_{EM,t} \leq 1$) is compared to the observation (y_t). If the tth observation is an event (or non-event) then $y_t = 1$ (or $y_t = 0$).

$$BS = \frac{1}{n} \sum_{t=1}^{n} (f_{EM,t} - y_t)^2 \qquad (1)$$

The Brier skill score (BSS) is formulated as a skill score related to a reference forecast, e.g. climatology in meteorology. In our case the reference forecast is based on the frequency of occurrence of events during the recorded forecast period (μ). A positive value of the BSS indicates that forecast is
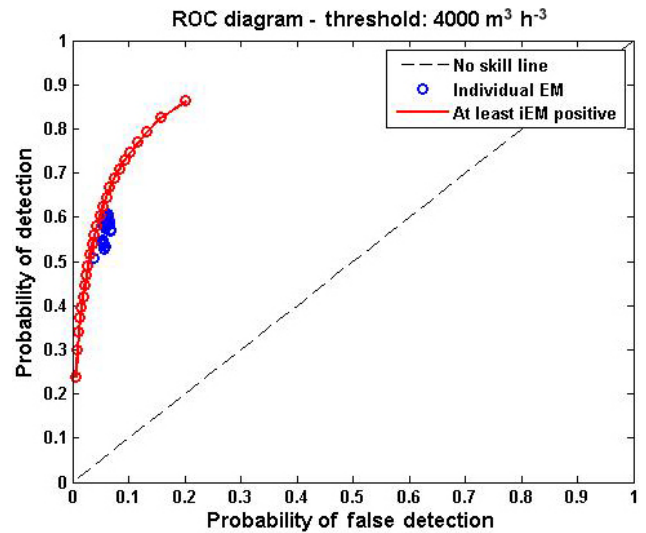

Figure 4. Example of a relative operating characteristic (ROC) diagram.

beneficial compared to the reference forecast.

$$BSS = 1 - \frac{BS}{BS_{ref}} \quad \text{with} \quad BS_{ref} = \frac{1}{n} \sum_{t=1}^{n} (\mu - y_t)^2 \qquad (2)$$

3.3 Relative operating characteristic (ROC)

The relative operating characteristic (ROC), which originates from signal detection theory (Mason, 1982), measures the discrimination ability (i.e. the ability to discriminate between events and non-events) of an EPS. The ROC plots the PoD versus the PoFD using a set of decreasing probability decision thresholds (Fig. 4). The selection of a lower decision threshold f_{EM} to convert the ensemble forecast to a single forecast is more conservative towards correctly predicting events. Therefore the PoD will be higher but the PoFD will increase as well.

The ROC diagram of the flow domain distinction using the weighted areal overlap NWP post-processing method is displayed in Fig. 4. The blue dots represent the discrimination skill of each individual EM. Figure 4 shows that all EMs have comparable discrimination skill. The red dots correspond to the discrimination skills from all decision thresholds, from $f_{EM} = 1$ at the bottom left (i.e. all EMs should

agree on the event occurrence) to $f_{EM} = \frac{1}{N}$ on the top right (i.e. the prediction of an event from a single EM is enough to consider an occurrence). Figure 4 underlines that EPSs and decision thresholds provide a larger range of available prediction skills than an EM individually. The choice of a decision threshold represents a trade-off between predicting events correctly and generating false alarms.

The skill score of a ROC diagram is calculated based on the area under the curve (ROCA). The ROCA ranges from 0 to 1, with a score of 1 corresponding to a perfect forecast and a score of 0.5 corresponding to the skill of a random forecast based on the probability of occurrence (μ).

3.4 Relative economic value (REV)

A proper evaluation of the benefits of a forecast system should not only consider the forecasts skill, e.g. using PoD and PoFD, or BSS. A detailed knowledge of the decision-making process is needed to answer the question: "how does this skill translate to an economic value of a forecast?". Furthermore, when using ensemble forecasts, the following question should be answered as well: "which decision threshold and NWP post-processing method for the EPS is the most beneficial for my purpose?".

The economic benefit from a forecast depends on the alternative courses of action and their consequences. Each course of action is associated with a cost and leads to economic benefit or loss depending on the observed outcome. The task is thus to choose the appropriate actions that will maximize the expected gain or minimize the expected loss. The usefulness of the forecast can thus be quantified by considering the occasions when the forecast was beneficial, detrimental or neutral with respect to the process of decision making.

The relative economic value of our urban hydrological prediction system is here inspired by the relatively simple cost–loss ratio decision model introduced by Richardson (2000). Richardson developed this approach to assess the economic value of taking costly actions to mitigate the consequences of forecast adverse weather events in order to reduce the potential loss associated with them. The decision threshold that can empirically be shown to lead to the lowest expense in the long term should be adopted. Richardson illustrated his approach for the problem of road gritting to prevent the formation of ice. Subsequently Roulin (2007) used this approach to investigate the benefit of river-flow mitigation measures for two catchments in Belgium, and Chang et al. (2015) applied it to assess the relevance of typhoon mitigation measures in Taiwan.

All these studies consider adverse events which can be mitigated at a cost, reducing the loss associated with these events, and their decision models are therefore based on a cost–loss ratio. This study investigates a different perspective. Instead of taking mitigating measures when adverse events are predicted, the system is optimized when no events are predicted in order to achieve a positive gain, and left un-

Table 3. Economical value assigned to the different outcomes of the contingency table (L: loss; G: gain).

	Event observed	
Event forecast	Yes	No
Yes	0	0
No	L	G

der its traditional management when events are predicted. Therefore, our decision model is based on a gain–loss ratio. During low-flow periods, when no events are forecast, the management objective is switched to energy consumption by utilizing the smart grid energy market, leading to a gain (G). As a consequence, mis-predicted high-flow events will jeopardize the IUDWS, e.g. the detention basins may not be empty in time. These negative outcomes are represented by a loss (L). In the case of forecast events (hits and false alarms), the management objectives of the IUDWS remain unchanged. The economic outcome of these two situations remains the same and therefore a null value is assigned to them; see Table 3.

Furthermore Richardson (2000) used a static ratio, the cost of mitigation measures and reduction of loss associated were fixed. This study encompasses the possibility of a time-dependent gain–loss ratio. Indeed, the gain (G) from switching the management objectives to energy optimization depends on the state of the energy market at the given time. Similarly, the loss (L) resulting from mis-predicted events is related to the current status of the IUWDS, e.g. the volume of water stored.

Based on Tables 2 and 3 the expected economic value of using the forecast for decision making over one time step (n represents the total number of time steps) can be expressed empirically as follows:

$$E_{forecast} = \frac{d \cdot G - c \cdot L}{n}. \tag{3}$$

In case of a perfect forecast ($b = c = 0$) the economic value would be as follows:

$$E_{perfect} = d \cdot \frac{G}{n} = (1 - \mu) \cdot G. \tag{4}$$

If no forecasts are available, the optimal course of action can be determined based on the empirical frequency of occurrence of an event, μ (climatological information in case of weather event as for Richardson, 2000). The two possible courses of action are either to always optimize the system despite the losses or to never optimize the system. $E_{statistic}$ considers the highest economic value between these two courses of action (Eq. 5); never optimizing (i.e. the IUDWS management is unchanged) would lead to an null economic value whereas always optimizing would lead to a gain G associated

to a loss L when events do occur.

$$E_{\text{statistic}} = \max(G - \mu \cdot L, 0) \tag{5}$$

The relative economic value (REV), as defined by Richardson (2000), compares the benefit of acting on a given forecast to the benefit which would be achieved by acting on a perfect forecast as a ratio (Eq. 6).

$$\text{REV} = \frac{E_{\text{forecast}} - E_{\text{statistic}}}{E_{\text{perfect}} - E_{\text{statisic}}} \tag{6}$$

The REV expressed by Eq. (6) can be reformulated using Eqs. (3), (4) and (5) and expressed as a function of the PoD, the PoFD, the frequency of occurrence (μ) and the gain–loss ratio ($\alpha = \frac{G}{L}$) as shown by Eq. (7) and displayed in Fig. 5.

$$\text{REV} = \tag{7}$$
$$\frac{\alpha \cdot (1 - \mu) \cdot (1 - \text{PoFD}) - (1 - \text{PoD}) \cdot \mu - \max(\alpha - \mu, 0)}{\alpha \cdot (1 - \mu) - \max(\alpha - \mu, 0)}$$

The possible value of the REV ranges from 1, corresponding to a perfect forecast, to minus infinity. In case of positive REV the use of the forecast is beneficial, whereas a negative REV indicates that using statistical information and either always or never optimizing the IUDWS yields a better economic value than using the weather forecast. Hence the REV can be divided in 3 domains: (i) the interval on the right of the curve in which it is preferable to always optimize (dotted domain on the right side of Fig. 5), (ii) the interval with positive REV covered by the curve in which using the forecast is beneficial (middle domain in Fig. 5) and (iii) the interval on the left in which it is preferable to never optimize (crosshatched domain on the left side of Fig. 5). Assuming that a perfect knowledge of the future yields a benefit β (compared to purely statistical information), then using the actual forecast provides a benefit to the user of $(100 \cdot \text{REV}) \%$ of β.

Figure 6 displays the ROC diagram and the REV-α relationship for flow forecast based on the catchment weighted areal overlap post-processing method. As explained in Sect. 3.3. the ROC diagram describes the EPS forecast discrimination skill for the different decision thresholds, f_{EM}. To support decision making the ROC diagram is converted to the REV-α relationship. Each point of the ROC diagram (Fig. 6a) represents a discrimination skill (PoD, PoFD) for a given decision threshold based on the fraction of EMs predicting an event (f_{EM}). For each of these points the REV can be determined as a function of the gain–loss ratio α (Eq. 7 and Fig. 5).

4 Results and discussion

4.1 ROC, REV and NWP post-processing methods.

The REV is closely related to the ROC diagram as indicated by Richardson (2000); Zhu et al. (2002) and illustrated in
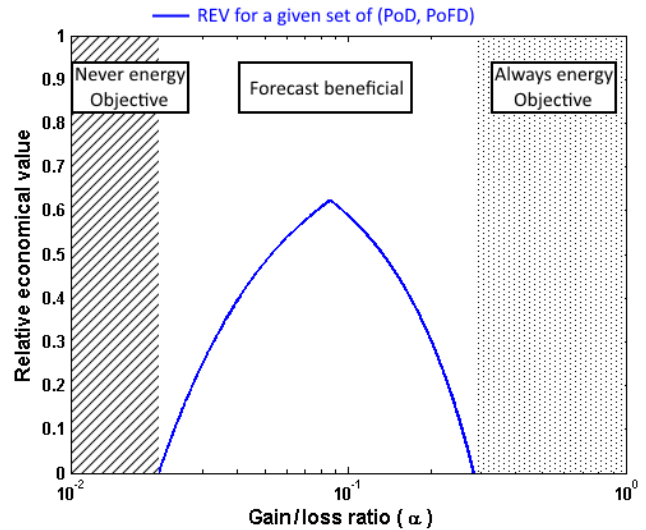

Figure 5. The 3 domains of operation of the REV curve as a function of the gain–loss ratio α.

Fig. 6. The curves in Fig. 6b show the REV-α relationship for the decision thresholds (f_{EM}) highlighted in Fig. 6a. The green dot (number 5) in Fig. 6a corresponds to a decision threshold $f_{\text{EM}} = 1/25$ and provides the highest PoD for this EPS; the REV associated with it, i.e. the green line (number 5) in Fig. 6b, leads to the highest REV for low α values (below 0.105) which corresponds to a high negative impact of missed events. Other decision thresholds yield better REV for higher α, e.g. the decision threshold $f_{\text{EM}} = 5/25$ corresponding to the red dot (legend 4) in Fig. 6a provides the highest REV (legend 4) for α within the range [0.16; 0.18]. Hence as demonstrated by Richardson (2000) the ensemble has better discrimination and can provide higher REV to a wider range of users (i.e. larger interval with positive REV) than any individual deterministic forecast (colour line) as illustrated by the envelope curve.

The implementation of the IUDWS energy consumption optimization scheme is challenged by potentially missed high-flow events. Indeed, these situations would lead to inappropriate management, jeopardizing the performance of the IUDWS. As explained in Sect. 2.2, post-processing methods can be applied to enhance the NWP, e.g. by accounting for potentially misplaced events which can have significant impact at an urban hydrology scale. Figure 7 displays the result considering the NWP maximal threat post-processing EPS method with a 6-grid-cell radius around the catchment. This approach is more conservative towards avoiding missed events and yields higher PoD at the cost of higher PoFD, which extends the ROC diagram. The ROC curves in Fig. 7a show that the two approaches are complementary; the areal overlap method provides better discrimination skill for low PoFD whereas the maximal threat EPS post-processing method provides better discrimination skill for higher PoFD.
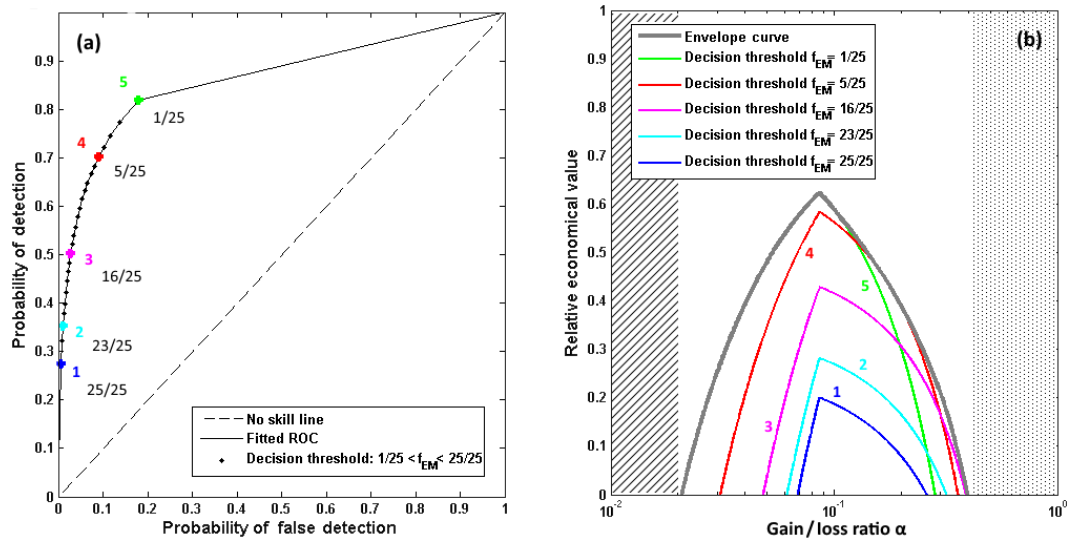
Figure 6. ROC and REV diagram for flow domain forecast based on catchment weighted areal overlap.
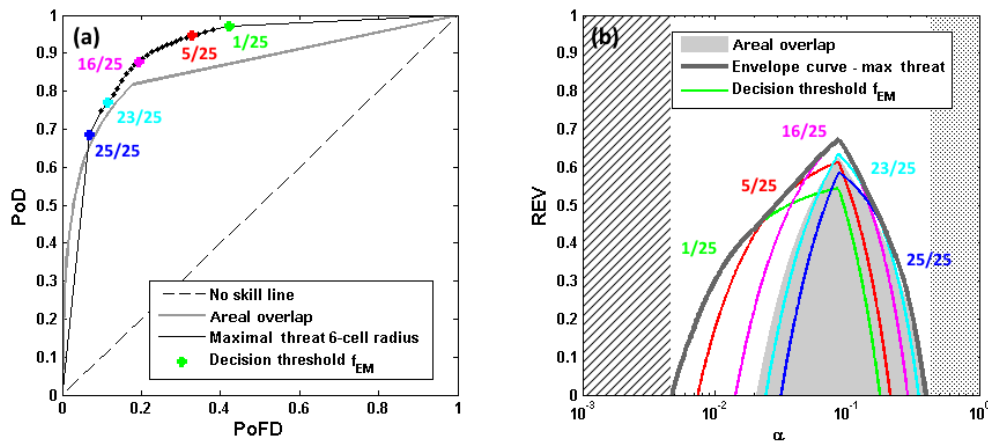

Figure 7. ROC and REV diagram for flow forecasts considering the two NWP post-processing methods: the maximal threat EPS method with a neighbourhood radius of 6 grid cells in colour and the catchment weighted areal overlap method in grey colour as background.

The ROCA of each approach is respectively 0.86 and 0.91 and the ROCA merging both approaches is 0.92.

This new ROC curve results in the extension of the α-interval with positive REV which characterizes the range of beneficial forecast use (Fig. 7b). To ease the comparison the area under the envelope curve of the areal overlap approach is displayed in grey colour as background in Fig. 7b, and Table 4 gives intervals of positive α for both approaches. The weighted areal overlap provides a slightly better upper bound whereas the maximal threat approach significantly expands the interval of positive REV for low α values. Therefore, using this NWP post-processing approach increases the range of beneficial forecast usages.

The comparison between these two NWP-post processing approaches using the Brier Skill Score (BSS) shows a deterioration of the forecast skill when using the maximal threat

approach, which has a negative BSS indicating that the forecast performs worse than the reference forecast based on the frequency of occurrence of an event (μ). This decrease in performance can be explained by an increase in false alarms due to the precautions towards not missing a major rain event of this approach. This result underlines the need for an economical assessment rather than purely forecast skills to draw conclusions of the usefulness of a forecast for a given decision making situation.

4.2 Examples of EPS flow domain prediction

In order to illustrate the different situations of decision making taken as a starting point for this paper (i.e. when to switch from flow management to energy management and vice versa) a range of 4 theoretical α-values were consid-

www.hydrol-earth-syst-sci.net/21/2531/2017/

Hydrol. Earth Syst. Sci., 21, 2531–2544, 2017

Table 4. BSS and REV characteristics for the two different NWP post-processing methods.

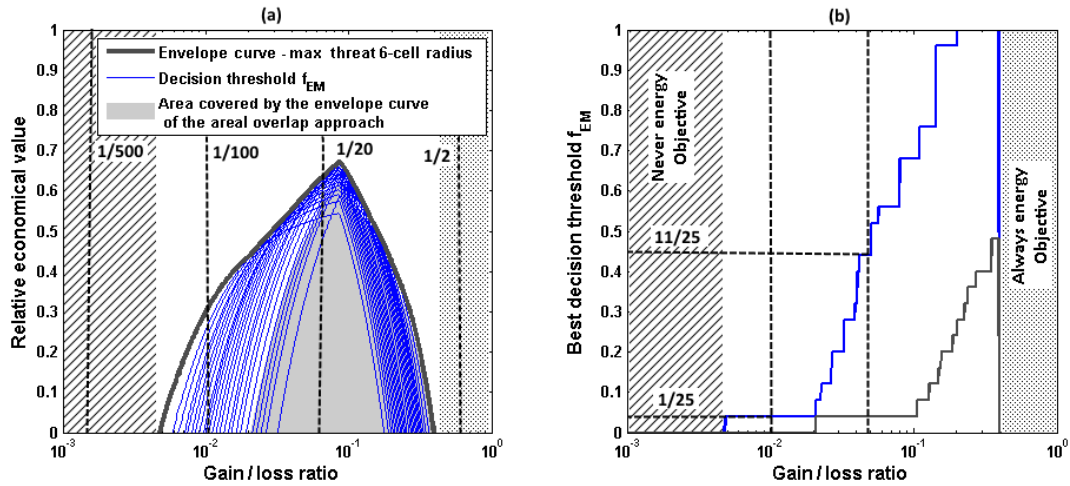|	ROCA	α-interval		BBS
		Lower bound	Upper bound	
Weighted areal overlap	0.86	0.0208	0.3955	0.14
Maximal threat 6-cell radius	0.91	0.0049	0.3940	−1.52

Figure 8. REV curves for the EPS NWP post-processing maximal threat in a radius of 6 grid cells from the catchment (**a**, left plot) and best decision threshold according to the α-value (**b**, right plot), in blue for the maximal threshold approach and in grey for the areal overlap approach.

Table 5. Decision threshold and REV for the theoretical 4 α-values considered, using the maximal threat post-processing method.

α	REV	Prediction criteria	
		Decision Threshold	NWP post-processing
1/2	Negative	Always energy objective	
1/20	0.59	$f_{EM} = 11/25$	Maximal Treat EPS
1/100	0.30	$f_{EM} = 1/25$	Maximal Treat EPS
1/500	Negative	Never energy objective	

ered, Table 5. The two outer α-values yield negative REV indicating that using the forecast data is not beneficial in these cases. The two other α-values yield positive REV indicating that using the forecast is beneficial in these cases. The decision threshold (f_{EM}) generating the highest relative benefit based on empirical data are displayed in Fig. 8 and in Table 5.

The coupled hydro-meteorological model provides an ensemble prediction of the flow at the catchment outlet for the incoming 2 days. Figure 9 provides an example of prediction. The first panel, Fig. 9a, displays the energy market during those two days, providing insight in the variation of the energy price and the CO_2 footprint through the proportion of wind energy. The shown data are based on historical val-

ues but similar information are available in real time on the electric smart grid. The fluctuation of the energy market for both parameters (Fig. 9a) illustrates the variation of the α-value in relation to the potential gain during a given period. During the first day (29 April 2015) the energy price ranges from 24 to 32 € MWh^{-1} and the proportion of wind energy varies from 15 to 49 %, whereas during the second day (30 April 2015) the energy price range from 23 to 41 € MWh^{-1} and the proportion of wind energy varies from 1 % to above 53 %. Hence the switch of consumption of 1 MWh can yield up to EUR 8 during the first day and up to EUR 18 during the second day. For comparison, the energy consumption per m^3 treated at Damhuså WWTP in 2015 was 0.261 kWh m^{-3} and in average 20 000 m^3 are treated during a dry day. Pumping and aeration of the biological treatment are the dominating energy users. The aeration of the bioreactor represents between 50 and 70 % of process energy consumption and largely depends on the inflow/load to the WWTP (Aymerich et al., 2015). The potential for energy switch highly dependents to the storage volume available upstream.

The North Pool Energy Market DK2, covering the Copenhagen area, has a Pearson correlation coefficient of −0.52 between energy price and proportion of wind energy in 2015, indicating a moderate negative linear relationship. Hence energy consumption optimizations based on economic objectives could also yield environmental benefits and vice versa.
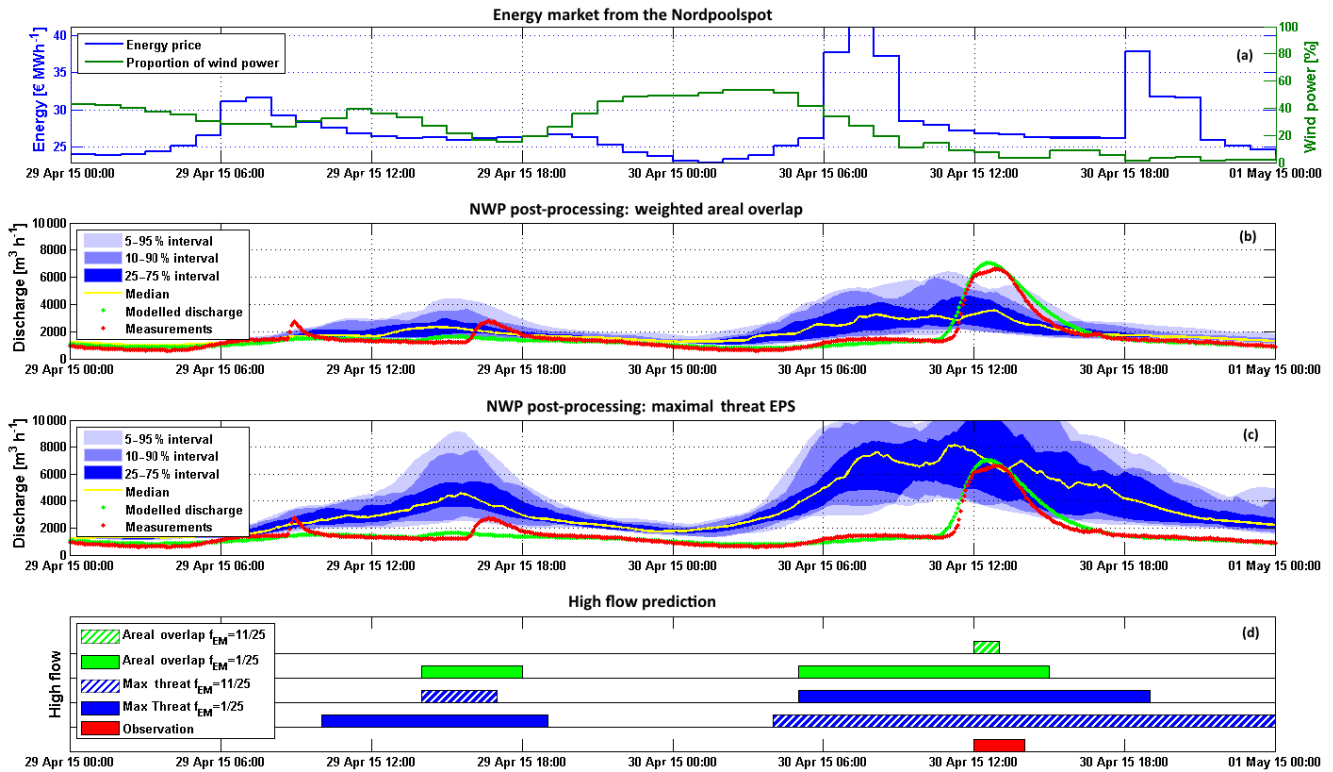
Figure 9. Example illustration of the EPS flow prediction system for 2 selected days, 29–30 April 2015. Energy market parameters, energy price and proportion of wind power (1, **a**), ensemble flow predictions using the areal average (**b**) and maximal threat (**c**) post-processing methods, and (**d**) flow domain predictions for the two post-processing methods and for each two decisions thresholds; cf. Table 5 (coloured areas imply that an event is predicted, otherwise not).

However it should be noticed that the control of the energy consumption based on the energy market can results in a decrease of the expenses together with an increase of the overall energy consumption as observed in Aymerich et al. (2015).

Figure 9b represents the flow forecast based on the catchment weighted areal overlap approach and Fig. 9c represents the flow forecast based on the maximal threat EPS approach with a 6-grid-cell radius. The measured flow during this period shows two minor rain events without significant flow impact the first day and a major rain event leading to high flows exceeding the $4000 \, \mathrm{m^3 \, h^{-1}}$? in the IUDWS the second day. Figure 9b illustrates the difficulty of the prediction to have a correct timing, most EMs predict the high-flow event but often too early. It can be noticed that due to the conservativeness of this second approach the EPS plume of flow forecasts overestimates the observed flow (in red), which explains the worsening of the BSS when using this approach.

The best flow domain predictions, considering a given α, is provided by the decision threshold defined using the REV method presented in Sect. 3.4. As displayed in Table 5, the highest REV for $\alpha = 1/20$ (respectively $\alpha = 1/100$) is achieved using the NWP post-processing approach "Maximal Threat EPS" with $f_{\mathrm{EM}} = \frac{11}{25}$ (respectively $f_{\mathrm{EM}} = \frac{1}{25}$). The flow domain predictions based on these criteria and on

the EPS flow forecast displayed in Fig. 9b and c are shown by the blue hatched (respectively plain blue) colour in Fig. 9d.

4.3 Outlooks

As mentioned in Sect. 4.2, the potential benefit from the energy consumption optimization management is largely conditioned by the storage volume available upstream. A major project is currently under implementation to comply with new regulations on CSO. Two large pipes will be constructed just before the inlet of the WWTP with a volume equivalent to the daily dry weather flow to the WWTP. This large storage volume, soon available upstream from the WWTP, provides an opportunity for real world implementation of the concept developed in this paper. Halvgaard et al. (2017) present a model predictive control (MPC) to control the power consumption of pumps in a sewer system and the treatment power consumption according to electricity prices and effluent quality (nitrogen) based on a case study at Kolding. The controller is able to balance electricity costs and treatment quality during predicted dry weather flow periods.

The predictions and therefore the skills of the EPS are based on a coupled meteorological and hydraulic model. This study used a lumped conceptual hydraulic model; a

more detailed hydrological model, including stochastic processes and on-line assimilation of flow measurements, might improve the prediction and thereby improve the REV further. Similarly, NWP models are continuously improving and benefit from the constant increase of computational calculation power to enhance their resolution and ensemble size. The techniques of data assimilation from radar measurement into NWP models are also consistently improving (Korsholm et al., 2015). Weather services are collaborating to continuously improve their meteorological models. For example, the HIRLAM consortium which developed the model structure of the DMI-HIRLAM-S05 NWP used in this study is currently developing and launching the non-hydrostatic convection-permitting HARMONIE model in cooperation with Météo-France and ALADIN, and EPSs with forecast horizons of up to 2 weeks are also available at the European level (http://www.ecmwf.int/). Therefore the accuracy and lead time of the prediction, and hence the potential benefit from the framework developed in this article, are expected to increase in the future.

Additionally, other characteristics of NWP can be utilized. The DMI-HIRLAM-S05 model, for example, generates a new 54 h EPS forecast every 6 h, and thereby the successive forecasts are overlapping each other. The forecast consistency, or in reverse the "forecast jump", provides valuable information on forecast uncertainty which could be utilized in the decision-making process. For example, the time-lagged method (Mittermaier, 2007) uses consecutive forecast overlapping to extend the EPS and enhance the predictions (i.e. the horizon of the forecast is reduced but its ensemble size is increased). This may increase the range of positive REV and allow use of the concept for decisions related to other problems than the energy optimization problem studied here.

Control systems can be decomposed into different layers in a hierarchy. Mollerup et al. (2016) presents a methodological approach to the design of optimized control strategies for sewer systems. The framework presented in this paper targets the upper layer of the hierarchy presented by Mollerup et al. (2016): the management of objectives where switching between different operational modes may take place. Completely different optimizing control strategies, including model predictive control techniques, may then run under different operation conditions – such as the "flow control" and "energy optimization" operational modes considered in this paper. Implementing such a switching system in practice requires that the gain–loss ratio expressing the economic consequences associated with the outcomes of the different courses of action used for the REV is quantified, which requires further research on monetization of non-market goods (e.g. CO_2 footprint or the environmental impact of CSOs) and may depend on local circumstances.

5 Conclusions

An ensemble flow prediction system for an IUDWS was developed using the DMI-HIRLAM-S05 EPS as input to a hydrological model. This system was tested on an urban catchment in the Copenhagen area based on recorded rainfall forecasts and flow data for the period from June 2014 to May 2016. Ensemble forecasting requires adaptation of the management rules in order to use probability forecasts instead of a deterministic forecast. The usefulness of the forecast should be evaluated not only based on its quality in terms of traditional skill scores but also based on its economic value for the daily decision-making process of the forecast user considered. The decision problem considered here is the switch from normal flow management during high-flow periods (wet weather) to smart grid energy optimization during low-flow periods (dry weather).

This article presents a framework to support decision making based on the prediction of the occurrence or lack of occurrence of an event using an EPS. The outcomes (gain for positives and loss for negatives) of the different possible courses of action are valued to determine the REV of using the forecast. The REV is closely related to the ROC diagram, which assesses the range of discrimination skills of an ensemble forecast. Hence, a REV curve, as a function of the gain / loss ratio α, can be generated for each probability threshold (f_{EM}) of the EPS. This method was developed in order to switch the IUDWS management objective from flow management to energy optimization, utilizing the electric smart grid when low-flow periods are predicted. This approach is based on daily optimization when non-events (dry weather) are forecast and differs from previous studies based on the REV concept, which investigated mitigation measures taking place when adverse events are forecast (e.g. flood, tornado) using a cost–loss ratio. In our approach for a given gain–loss ratio α, the probability threshold (f_{EM}) corresponding to the highest REV, symbolized by the envelope curve, should be applied to maximize the benefit of the optimization scheme. If the gain–loss ratio is outside the range of positive REV, then using the forecast is not beneficial. The gain–loss ratio α is a function of the potential gain from utilizing the variation of the smart grid energy market, which varies in time.

Two NWP post-processing methods were tested: (i) a realistic approach based on the weighted areal overlap between the NWP grid cells and the hydrological catchment, and (ii) a more conservative approach considering the maximal rainfall threat in the catchment vicinity. The second approach leads to a deterioration of classic forecast validation scores such as BSS due to a significant increase in the number of false alarms. However, this approach proves to be beneficial in regard to the decision-making process, especially when considering a low gain–loss ratio α for which missed forecast events are highly detrimental. Indeed, the maximal threat NWP neighbourhood post-processing method improves the

range of discrimination skill of the predictions shown on the ROC diagram and therefore provides a larger range of positive REV, increasing the range of beneficial forecast usage. This underlines the importance of assessing the forecast usefulness based on its potential economic value rather than solely on the usual forecast skills.

References

Atger, F.: Verification of intense precipitation forecasts from single models and ensemble prediction systems, Nonlin. Processes Geophys., 8, 401–417, doi:10.5194/npg-8-401-2001, 2001.

Aymerich, I., Rieger, L., Sobhani, R., Rosso, D., and Corominas, L.: The difference between energy consumption and energy cost: Modelling energy tariff structures for water resource recovery facilities, Water Res., 81, 113–123, doi:10.1016/j.watres.2015.04.033, 2015.

Bacher, P., Madsen, H., and Nielsen, H. A.: Online short-term solar power forecasting, Sol. Energy, 83, 1772–1783, doi:10.1016/j.solener.2009.05.016, 2009.

BIOFOS: Miljøberetning, Copenhagen, available at: http://www.biofos.dk/wp-content/uploads/2014/11/Miljoeberetning-2015.pdf (last access: 1 April 2017), 2015.

Bjerg, J. E., Grum, M., Courdent, V., Halvgaard, R., Vezzaro, L., and Mikkelsen, P. S.: Coupling of Weather Forecasts and Smart Grid-Control of Wastewater inlet to Kolding WWTP (Denmark), in: 10th International Urban Drainage Modelling Conference, 47–59, Mont Sainte-Anne, Québec, Canada, 2015.

Brier, G. W.: Verification of forecasts expressed in terms of probability, Mon. Weather Rev., 78, 1–3, doi:10.1175/1520-0493(1950)078<0001:VOFEIT>2.0.CO;2, 1950.

Chang, H.-L., Yang, S.-C. and Yuan, H.: Analysis of the Relative Operating Characteristic and Economic Value Using the LAPS Ensemble Prediction System in Taiwan, Mon. Weather Rev., 143, 1833–1848, doi:10.1175/MWR-D-14-00189.1, 2015.

Collischonn, W., Morelli Tucci, C. E., Clarke, R. T., Chou, S. C., Guilhon, L. G., Cataldi, M., and Allasia, D.: Medium-range reservoir inflow predictions based on quantitative precipitation forecasts, J. Hydrol., 344, 112–122, doi:10.1016/j.jhydrol.2007.06.025, 2007.

Courdent, V., Grum, M., and Mikkelsen, P. S.: Distinguishing high and low flow domains in urban drainage systems 2 days ahead using numerical weather prediction ensembles, J. Hydrol., doi:10.1016/j.jhydrol.2016.08.015, in press, 2017.

Cuo, L., Pagano, T. C., and Wang, Q. J.: A Review of Quantitative Precipitation Forecasts and Their Use in Short- to Medium-Range Streamflow Forecasting, J. Hydrometeorol., 12, 713–728, doi:10.1175/2011JHM1347.1, 2011.

Damrath, U., Doms, G., Frühwald, D., Heise, E., Richter, B., and Steppeler, J.: Operational quantitative precipitation forecasting at the German Weather Service, J. Hydrol., 239, 260–285, doi:10.1016/S0022-1694(00)00353-X, 2000.

Du, J.: Uncertainty and Ensemble Forecast, National Weather Service, available at: http://www.nws.noaa.gov/ost/climate/STIP/STILecture1.pdf (last access: 1 April 2017), 2007.

Feddersen, H.: A Short-Range Limited Area Ensemble Prediction System, Danish Meteorological Institute, Copenhagen, available at: http://www.dmi.dk/fileadmin/Rapporter/TR/tr09-14.pdf (last access: 1 April 2017), 2009.

Giebel, G., Badger, J., Landberg, L., Nielsen, H. A., Nielsen, T. S., Madsen, H., Sattler, K., Feddersen, H., Vedel, H., Tøfting, J., Kruse, L. and Voulund, L.: Wind power prediction using ensembles, Roskilde, available at: http://orbit.dtu.dk/files/57134275/ris_r_1527.pdf (last access: 1 April 2017), 2005.

Hadjsaïd, N. and Sabonnodiere, J.-C.: Smart Grids, First, ISTE Ltd, London UK, 2012.

Halvgaard, R., Vezzaro, L., Mikkelsen, P. S., Grum, M., Munk-Nielsen, T., Tychsen, P., and Madsen, H.: Integrated Model Predictive Control of Wastewater Treatment Plants and Sewer Systems in a Smart Grid, 1–16, Control Eng. Pract., submitted, 2017.

Harremoës, P., Pedersen, C. M., Laustsen, A., Sørensen, S., Laden, B., Friis, K., Andersen, H. K., Linde, J. J., Mikkelsen, P. S., and Jakobsen, C.: Funktionspraksis for afløbssystemer under regn., IDA Spildevandskomiteen, 2005.

Jørgensen, H. K., Rosenorn, S., Madsen, H., and Mikkelsen, P. S.: Quality control of rain data used for urban runoff systems, Water Sci. Technol., 37, 113–120, 1998.

Korsholm, U. S., Petersen, C., Sass, B. H., Nielsen, N. W., Jensen, D. G., Olsen, B. T., Gill, R., and Vedel, H.: A new approach for assimilation of 2D radar precipitation in a high-resolution NWP model, Meteorol. Appl., 22, 48–59, doi:10.1002/met.1466, 2015.

Laloy, E. and Vrugt, J. A.: High-dimensional posterior exploration of hydrologic models using multiple-try DREAM (ZS) and high-performance computing, Water Resour. Res., 48, 1–18, doi:10.1029/2011WR010608, 2012.

Langergraber, G., Alex, J., Weissenbacher, N., Woerner, D., Ahnert, M., Frehmann, T., Halft, N., Hobus, L., Plattes, M., Spering, V., and Winkler, S.: Generation of diurnal variation for influent data for dynamic simulation, Water Sci. Technol., 57, 1483–1486, doi:10.2166/wst.2008.228, 2008.

Leu, S.-Y., Rosso, D., Larson, L. E., and Stenstrom, M. K.: Real-time aeration efficiency monitoring in the activated sludge process and methods to reduce energy consumption and operating costs, Water Environ. Res., 81, 2471–2481, doi:10.2175/106143009X425906, 2009.

Mason, I.: A model for assessment of weather forecasts, Aust. Met. Mag., 30, 291–303, 1982.

Ministry of Foreign Affairs of Denmark: Independent from fossil fuels by 2050, available at: http://denmark.dk/en/green-living/strategies-and-policies/independent-from-fossil-fuels-by-2050, last access: 1 April 2017.

Mittermaier, M. P.: Improving short-range high-resolution model precipitation forecast skill using time-lagged ensembles, Q. J. Roy. Meteor. Soc., 133, 1487–1500, doi:10.1002/qj.135 , 2007.

Mollerup, A. L., Mikkelsen, P. S., and Sin, G.: A method-ological approach to the design of optimising control strate-gies for sewer systems, Environ. Model. Softw., 83, 103–115, doi:10.1016/j.envsoft.2016.05.004, 2016.

Nash, S. E.: The Form of the Instantaneous Unit Hydrograph, IASH Publ., 114–121, 1957.

Pappenberger, F., Scipal, K., and Buizza, R.: Hydrological as-pect of meteorological verification, Atmos. Sci. Lett., 9, 43–52, doi:10.1002/asl.171, 2008.

Richardson, D. S.: Skill and relative economic value of the ECMWF ensemble prediction system, Q. J. Roy. Meteor. Soc., 126, 649–667, 2000.

Rosso, D. and Stenstrom, M. K.: Comparative economic anal-ysis of the impacts of mean cell retention time and deni-trification on aeration systems, Water Res., 39, 3773–3780, doi:10.1016/j.watres.2005.07.002, 2005.

Roulin, E.: Skill and relative economic value of medium-range hy-drological ensemble predictions, Hydrol. Earth Syst. Sci., 11, 725–737, doi:10.5194/hess-11-725-2007, 2007.

Shrestha, D. L., Robertson, D. E., Wang, Q. J., Pagano, T. C., and Hapuarachchi, H. A. P.: Evaluation of numerical weather pre-diction model precipitation forecasts for short-term streamflow forecasting purpose, Hydrol. Earth Syst. Sci., 17, 1913–1931, doi:10.5194/hess-17-1913-2013, 2013.

Sun, J., Xue, M., Wilson, J. W., Zawadzki, I., Ballard, S. P., Onvlee-Hooimeyer, J., Joe, P., Barker, D. M., Li, P. W., Golding, B., Xu, M. and Pinto, J.: Use of nwp for nowcasting convective precip-itation: Recent progress and challenges, B. Am. Meteorol. Soc., 95, 409–426, doi:10.1175/BAMS-D-11-00263.1, 2014.

Theis, S. E., Hense, A., and Damrath, U.: Probabilistic precipitation forecasts from a deterministic model: a pragmatic approach, Me-teorol. Appl., 12, 257, doi:10.1017/S1350482705001763, 2005.

Unden, P., Rontu, L., Jarvinen, H., Lynch, P., Calvo, J., Cats, G., Cuxart, J., Eerola, K., Fortelius, C., Garcia-moya, J. A., Jones, C., Lenderlink, G., Mcdonald, A., Mcgrath, R., and Navascues, B.: HIRLAM-5 Scientific Documentation, Norrkoping, available at: http://hirlam.org/index.php/component/docman/doc_view/270-hirlam-scientific-documentation-december-2002?Itemid=70 (last access: 1 April 2017), 2002.

Weron, R.: Modeling and forecasting electricity loads and prices: A statistical approach, First Edn., John Wiley & Sons Ltd., 2006.

Wilks, D. S.: Statistical Methods in the Atmospheric Sciences, El-sevier, 2011.

WWRP/WGNE: Recommendations for the Verification and Inter-comparison of QPFs and PQPFs from Operational NWP Models, Geneva, Switzerland, available at: http://www.wmo.int/pages/prog/arep/wwrp/new/documents/WWRP2009-1_web_CD.pdf (last access: 1 April 2017), 2009.

Zhu, Y., Toth, Z., Wobus, R., Richardson, D., and Mylne, K.: The economic value of ensemble–based weather forecasts, B. Am. Meteorol. Soc., 83, 73–83, 2002.

Zugno, M.: Optimization under uncertainty for management of renewables in electricity markets, University of Denmark, available at: http://orbit.dtu.dk/en/publications/optimization-under-uncertainty-for-management-of-renewables-in-electricity-markets(d314a0c4-185f-4983-95ff-21133defd41d).html (last access: 1 April 2017), 2013.